Atherosclerosis 294 (2020) 25–32

Contents lists available at ScienceDirect

Atherosclerosis

journal homepage: www.elsevier.com/locate/atherosclerosis

Performance of a deep learning algorithm for the evaluation of CAD-RADS classification with CCTA

Giuseppe Muscogiuri[a,1], Mattia Chiesa[a,1], Michela Trotta[b], Marco Gatti[c], Vitanio Palmisano[d], Serena Dell'Aversana[e], Francesca Baessato[f], Annachiara Cavaliere[g], Gloria Cicala[h], Antonella Loffreno[i], Giulia Rizzon[g], Marco Guglielmo[a], Andrea Baggiano[a], Laura Fusini[a], Luca Saba[d], Daniele Andreini[a,j], Mauro Pepi[a], Mark G. Rabbat[k,l], Andrea I. Guaricci[m], Carlo N. De Cecco[n], Gualtiero Colombo[a], Gianluca Pontone[a,*]

[a] Centro Cardiologico Monzino, IRCCS, Milan, Italy
[b] Department of Electrical, Computer and Biomedical Engineering, University of Pavia, Pavia, Italy
[c] Department of Surgical Sciences, Radiology Institute, University of Turin, Turin, Italy
[d] Department of Medical Imaging, University of Cagliari, Monserrato, Italy
[e] Department of Advanced Biomedical Sciences, University of Naples "Federico II,", Naples, Italy
[f] Section of Cardiology, Department of Medicine, University of Verona, Verona, Italy
[g] Department of Medicine, Institute of Radiology, University of Padova, Padua, Italy
[h] Section of Radiology, Department of Medicine and Surgery, University of Parma, Parma, Italy
[i] Department of Cardiology, University of Insubria, Varese, Italy
[j] Department of Cardiovascular Sciences and Community Health, University of Milan, Italy
[k] Loyola University of Chicago, Chicago, IL, USA
[l] Edward Hines Jr. VA Hospital, Hines, IL, USA
[m] Institute of Cardiovascular Disease, Department of Emergency and Organ Transplantation, University Hospital "Policlinico Consorziale" of Bari, Bari, Italy
[n] Department of Radiology and Imaging Sciences, Emory University, Atlanta, GA, USA

HIGHLIGHTS

- Deep convolutional neural network (CNN) yielded accurate automated Coronary Artery Disease Reporting and Data System (CAD-RADS) classification in patients with suspicious CAD.
- CAD-RADS classification is significantly faster compared to human evaluation.
- CNN can reduce the time of CCTA reporting in the next future.

ARTICLE INFO

Keywords:
CADRADS
Convolutional neural network
Artificial intelligence
Coronary artery disease
Plaque characterization

ABSTRACT

Background and aims: Artificial intelligence (AI) is increasing its role in diagnosis of patients with suspicious coronary artery disease. The aim of this manuscript is to develop a deep convolutional neural network (CNN) to classify coronary computed tomography angiography (CCTA) in the correct Coronary Artery Disease Reporting and Data System (CAD-RADS) category.

Methods: Two hundred eighty eight patients who underwent clinically indicated CCTA were included in this single-center retrospective study. The CCTAs were stratified by CAD-RADS scores by expert readers and considered as reference standard. A deep CNN was designed and tested on the CCTA dataset and compared to on-site reading. The deep CNN analyzed the diagnostic accuracy of the following three Models based on CAD-RADS classification: Model A (CAD-RADS 0 *vs* CAD-RADS 1–2 *vs* CAD-RADS 3,4,5), Model 1 (CAD-RADS 0 *vs* CAD-RADS > 0), Model 2 (CAD-RADS 0–2 *vs* CAD-RADS 3–5). Time of analysis for both physicians and CNN were recorded.

Results: Model A showed a sensitivity, specificity, negative predictive value, positive predictive value and accuracy of 47%, 74%, 77%, 46% and 60%, respectively. Model 1 showed a sensitivity, specificity, negative predictive value, positive predictive value and accuracy of 66%, 91%, 92%, 63%, 86%, respectively. Conversely,

* Corresponding author. Centro Cardiologico Monzino, IRCCS, Via Carlo Parea 4, 20138, Milan, Italy.
E-mail address: gianluca.pontone@ccfm.it (G. Pontone).
[1] These authors contributed equally to this work.

https://doi.org/10.1016/j.atherosclerosis.2019.12.001
Received 21 August 2019; Received in revised form 1 December 2019; Accepted 6 December 2019
Available online 23 December 2019
0021-9150/

Model 2 demonstrated the following sensitivity, specificity, negative predictive value, positive predictive value and accuracy: 82%, 58%, 74%, 69%, 71%, respectively. Time of analysis was significantly lower using CNN as compared to on-site reading (530.5 ± 179.1 *vs* 104.3 ± 1.4 sec, $p = 0.01$)
Conclusions: Deep CNN yielded accurate automated classification of patients with CAD-RADS.

1. Introduction

Cardiac computed tomography angiography (CCTA) is an excellent non-invasive technique for the assessment of stable coronary artery disease (CAD) [1,2].

Thus, application of CCTA in clinical practice is rapidly increasing especially considering its potential role as a gatekeeper for invasive coronary angiography [3]. Several classification systems for reporting of CCTA have been created with the recent introduction of CAD-RADS [4].

In CAD-RADS classification, the final score of CCTA is based on patient based analysis. Each vessel is evaluated using the following scale: 0 = absence of CAD; 1 = stenosis between 1 and 24%; 2 = stenosis between 25 and 49%; 3 = stenosis between 50 and 69%; 4 = stenosis between 70 and 99% or > 50% left main or three vessels > 70%; 5 = total occlusion; N = non diagnostic studies.

The CAD-RADS classification affords to have a simple classification for CAD, identifying patients that may require additional functional testing or invasive angiography.

Furthermore, CAD-RADS classification has a pivotal role in terms of prognosis. Indeed, as shown by Xie et al., patients with CAD-RADS 5 showed a 5 year event significantly higher compared with CAD-RADS 0 [5].

Despite the majority of cardiac imaging interpretation and reporting being performed by readers, it is important to consider that machine learning or deep learning (DL) approaches may allow the evaluation of images in a short time compared to humans [6]. The application of artificial intelligence (AI) in cardiac imaging represents an interesting novelty in terms of both diagnosis and prognosis [7].

Convolutional neural networks (CNN) are the most powerful Deep Learning technique used for diagnostic classification and prediction, starting from medical images [8].

Considering the impact on clinical practice of CAD-RADS classification and the relative short time of analysis of the AI approach, we analyzed the effect of a novel CNN technique for CAD-RADS classification in patients referred for clinically indicated CCTA.

2. Materials and methods

2.1. Study population

We retrospectively analyzed the examinations of patients who underwent CCTA for clinical purposes from 2016 to 2018. Exclusion criteria were heart rate ≥80 bpm despite intravenous administration of beta blockers, atrial fibrillation and BMI ≥35 kg/m^2. The study was approved by the institutional ethical committee. All patients provided written informed consent.

2.2. CCTA acquisition and analysis

2.2.1. Patient preparation to CCTA and CCTA protocol

In patients with heart rate ≥65 bpm, without any contraindications to β-blockade therapy, metoprolol with a titration dose up to 25 mg was administered [9]. Sublingual nitrates were administered 5 min before the CCTA acquisition [10].

CCTA acquisition was acquired using the following two CT scanners: Discovery CT 750 HD and Revolution CT (GE Healthcare, Milwaukee, IL). In the CCTA protocol of Discovery CT 750 HD, the following CT protocols were used: slice configuration 64 × 0.625 mm, with adapted tube current and tube voltage based on patient's BMI [11].

The CCTA protocol with the Revolution CT (GE Healthcare, Milwaukee, IL) was based on the following parameters: slice configuration 256 × 0.625 mm with tube current and tube voltage based on BMI.

In both CT scanner protocols, 50–70 mL of contrast medium (Iomeron 400 mg/mL, Bracco, Milan, Italy) was administered through the antecubital vein at an infusion rate of 5 mL/s, followed by 50 mL of saline solution at the same infusion rate of contrast agent. In both CT scanners, CCTA was performed using the bolus tracking technique.

All images for both CT scanners were reconstructed using filtered back projection and in 75% or 40–80% of cardiac cycle based on the ECG-triggering acquisition used [12]. In selected cases with poor image quality, the dataset was reconstructed by using intracycle motion correction as previously described [12,13].

2.2.2. Image quality analysis

Subjective image quality was assessed by two cardiac imaging radiologists (VP and GM) with five and seven years of experience in cardiovascular imaging using the following four point Likert scale: 1 = non-diagnostic, 2 = adequate image quality, 3 = good image quality; 4 = excellent image quality.

Regarding objective image quality, the image noise was measured by manually drawing a region of interest (ROI) 20 mm in diameter in the aortic root, above the origin of the left main coronary artery (LM) and expressed as the standard deviation (SD) of vessel attenuation. Signal to noise ratio (SNR) for each coronary segment was calculated by dividing the coronary attenuation of proximal segments and image noise. Contrast to noise ratio (CNR) was obtained by dividing the difference between attenuation of coronary and surrounding tissue with the image noise [14].

Coronary arteries were analyzed using the segmentation model according to the American Heart Association (AHA) [15].

2.2.3. CAD-RADS score and coronary plaque evaluation

The pool of CCTA examinations was reconstructed then analyzed in consensus by five different random couples between 10 radiologists and cardiologists (GP, MG, MG, AB, SD, GP, VP, GR, AC, DA). The experience of the cardiac imagers involved in the analysis ranged from 5 to 10 years. A CAD-RADS score was attributed for each examination. In cases of disagreement, a cardiac imager (AIG) with ten years of experience in cardiovascular imaging adjudicated the final CAD-RADS score.

Based on composition of plaque, in patients with CADRADS > 0, coronary plaques were identified and classified as calcified, mixed and soft in all vessels [16].

Considering that CAD-RADS score is based on patient analysis, the burden of coronary artery disease of stenosis in other vessels was evaluated and classified according to the SCCT guidelines [17].

According to the CAD-RADS classification, the following three models were created: Model A = CAD-RADS 0 *vs* CAD-RADS 1–2 *vs* CAD-RADS 3–5. Subsequently, two models were derived from Model A: Model 1 = (CAD-RADS 0 *vs* CAD-RADS 1–5) and Model 2 = (CAD-RADS 0–2 *vs* CAD-RADS 3–5). Time of analysis for each CCTA analysis of CNN and on-site reading were recorded and compared.

2.3. Deep learning methods

2.3.1. Dataset generation

Each CCTA scan was stored in a DICOM format. For each sample, we removed the first 16 slices, selected the next (excluding the slices not

representing the heart), placed them in an 11x11 squared image and resized each image to 512x512 pixels.

Axial images were provided to CNN algorithm in the same cardiac phase used for the clinical reporting. All CCTA images did not include any annotation.

Finally, to increase and balance the number of samples (100 in each class) and to reduce the overfitting, we performed the data augmentation strategy, rotating and zooming images [18]. At the end, the dataset was composed of 6 classes, each one of 100 samples.

2.3.2. CNN architecture

The 2D-CNN used in this study was designed after testing several combinations of hyperparameters. The keras R package in the framework of Tensorflow was used to build and test the CNN. The convolutional section of the network consisted of three consecutive layers of blocks, each one containing a sequence of three convolutional layers (32 filters 3 x 3 px) and a max-pooling layer. Before each max-pooling layer, a batch normalization strategy was implemented to reduce the overfitting of the training model [19]. Each convolutional layer was composed of 32 filters (3 x 3 px) and the pooling windows size was 2 x 2. The number of neurons in the output layer corresponded to the number of classes in a specific classification analysis. To handle the overfitting, a dropout strategy was implemented before the first hidden layer (dropout rate: 0.5) [19]. The ReLU activation function [19] was used for each neuron (densely connected and convolutional ones), except for the output layer ones (activation function: 'softmax'). Finally, we used the Back Propagation optimizer to minimize the categorical cross entropy and implemented the 'early stopping' strategy as a regularization method to prevent overfitting. The designed CNN is sketched in Fig. 1.

The main endpoints of the study were:

a) Evaluation of diagnostic accuracy of CNN in Model A, Model 1 and Model 2.
b) Univariate and multivariate analysis for identification of predictive factors for failure of CNN were analyzed.
c) Comparison of time of analysis between CNN approach and on-site reading.

2.3.3. Statistical analysis

To evaluate the overall classification performance, a 5-fold Cross Validation was implemented (Fig. 2). For each iteration, a training set is generated, combining four folds (80 samples per class); the remaining fold (20 samples per class) was used as test set. The training set is used to learn the CNN parameters (Fig. 3 and Supplemental materials), while on the test set the standard evaluation metrics (i.e., sensitivity, specificity, negative predicted value, positive predicted value, and accuracy, and the area under the curve) are calculated.

Intra- and inter-observer reliability was calculated using the kappa score by considering all subjects and splitting subjects by class.

Univariate and multivariate logistic regression analyses were used to identify independent factors associated with a CNN misreading of the CAD-RADS score. A p-value < 0.05 was considered significant. Statistical analysis was performed using SPSS 25 (SPSS Inc, Chicago, IL) and R version 3.5.1 (R Foundation for Statistical Computing, Vienna, Austria).

3. Results

Two hundred eighty-eight patients were randomly extracted and evaluated (CAD-RADS 0: 50 exams; CAD-RADS 1: 50 exams; CAD-RADS 2: 50 exams; CAD-RADS 3: 50 exams; CAD-RADS 4: 50 exams; CAD-RADS 5: 38 exams). Four patients were excluded due to inadequate image quality. Two example cases of CAD-RADS 0 and CAD-RADS 5 are summarized in Fig. 3.

The baseline characteristics of the overall population are summarized in Table 1.

The subjective image quality was good for all coronary segments showing a high inter-reader and intra-reader reproducibility Tables 2 and 3.

The diagnostic accuracy of the 2D-CNN approach was analyzed for Model A, demonstrating a sensitivity, specificity, negative predictive

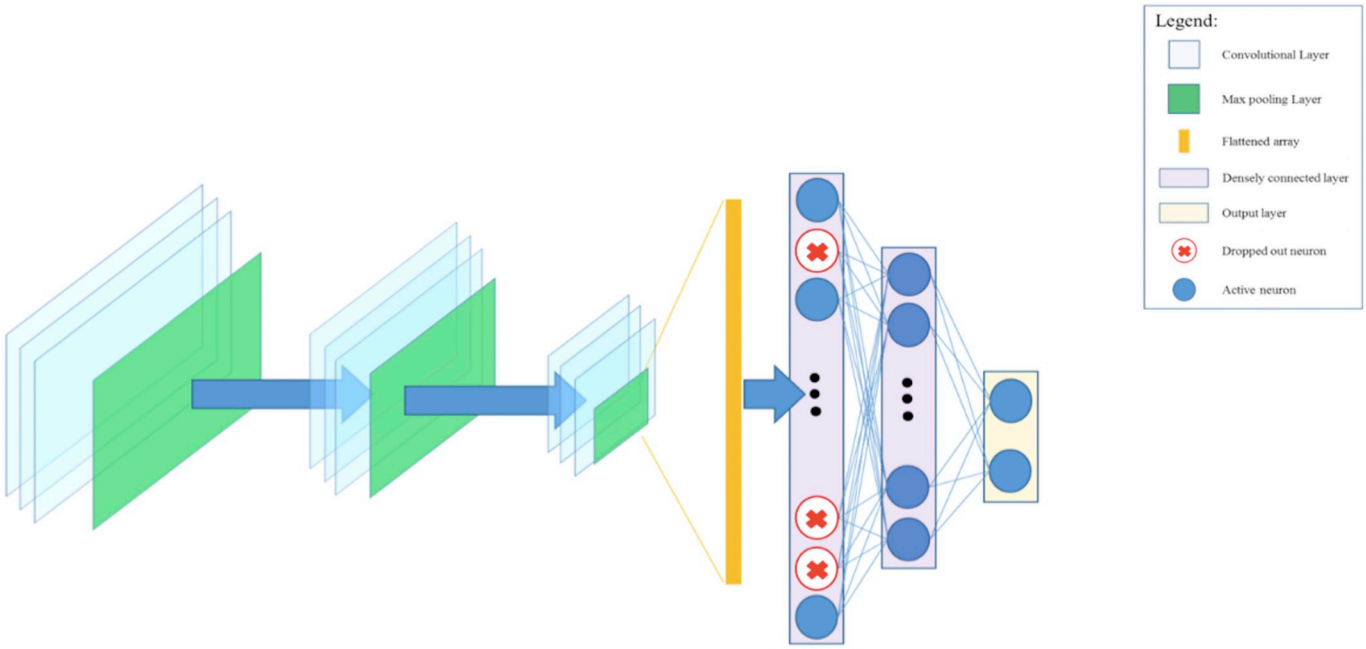

Fig. 1. Graphical sketch of the designed CNN architecture.
Three consecutive convolutional blocks, each one composed of 3 convolutional layers (light blue squares) and a max pooling layer (green square), are followed by a densely connected network (2 hidden layers (violet squares) and an output layer (yellow square)). During the CNN training, some neurons are dropped out (red crossed circles) and others are active (blue circles). (For interpretation of the references to colour in this figure legend, the reader is referred to the Web version of this article.)

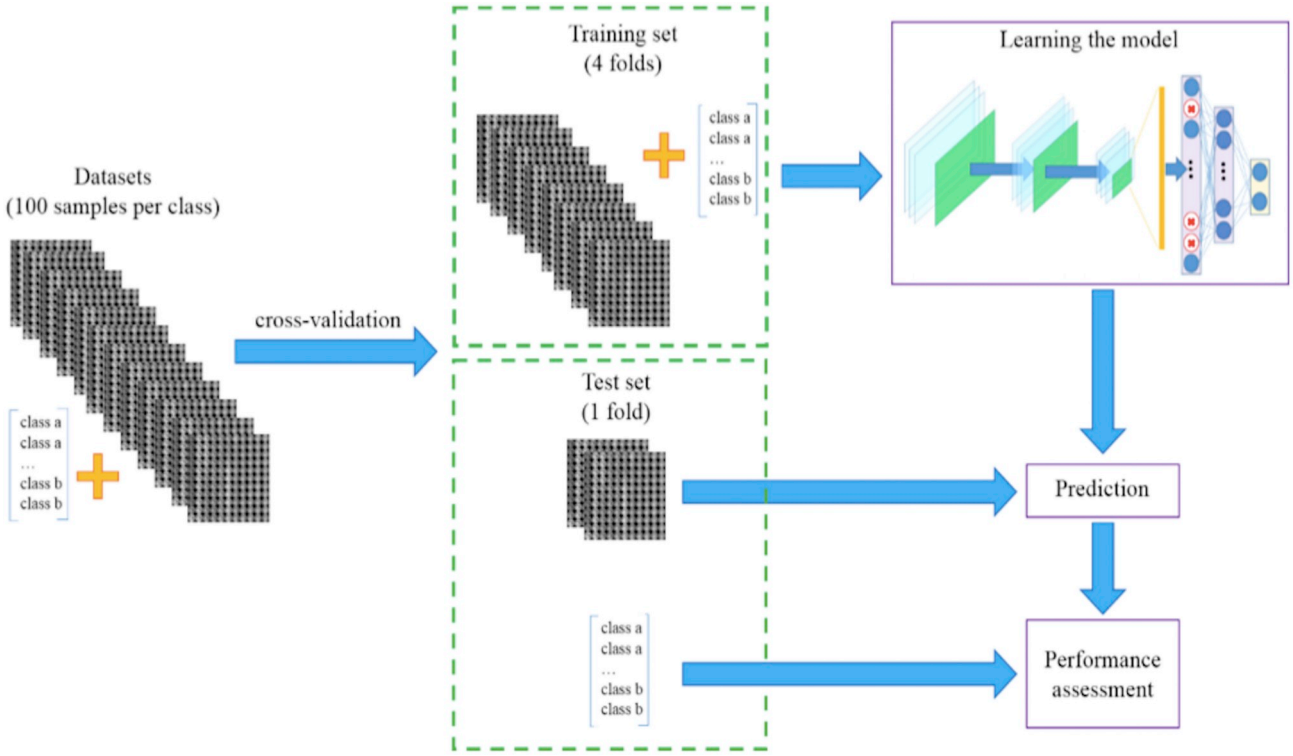

Fig. 2. Overview of the deep learning analysis.
First, the whole dataset was split in 5 folds, each one composed of 20 samples per class. Then, a cross validation procedure was implemented: 4 folds were selected to train the CNN (training set) and build the model; the fifth fold was used to test the learned model (test set) and to assess the performance.

value, positive predictive value and accuracy of 47% (20–74%), 74% (54–94%), 77% (68–86%), 46% (31–61%) and 60% (54–66%), respectively.

From Model A, two further models were derived, Model 1 and Model 2, showing a sensitivity, specificity, negative predictive value, positive predictive value, accuracy and area under curve of 66%

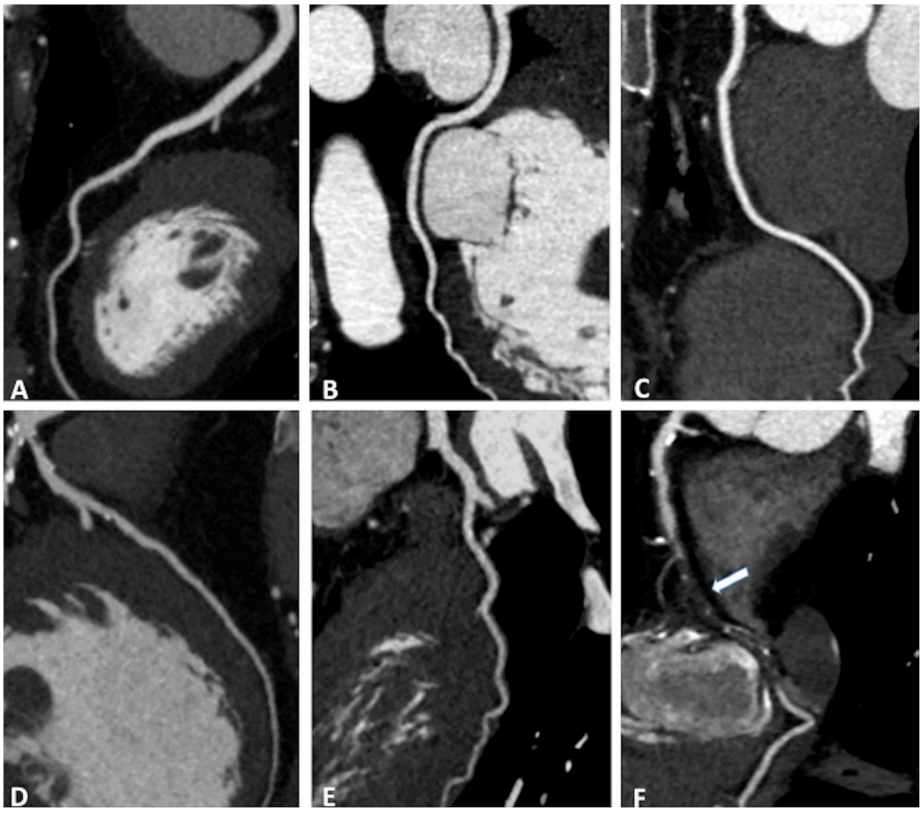

Fig. 3. Upper row: A 53-year-old woman with family history of cardiovascular disease, palpitations and dyspnea. CAD RADS 0: (A) absence of pathology in the left anterior descending artery, (B) circumflex artery and (C) right coronary artery. Lower row: A 67-year-old man with dyslipidemia and severe left ventricular dysfunction by echocardiography. CAD RADS 5: (D) severe stenosis of the proximal left anterior descending artery, (E) absence of pathology of circumflex artery and (F) occlusion of mid portion of right coronary artery (arrow).

Table 1
Baseline characteristics of the overall population.

Characteristics	Values
Number, *n*	288
Age (y), mean ± SD	60.6 ± 12.4
Male, *n* (%)	198 (69)
Body mass index (kg/m^2), mean ± SD	25.8 ± 4.5
Risk factors	
Hypertension, *n* (%)	96 (33)
Smoker, n (%)	46 (16)
Hyperlipidemia, *n* (%)	86 (30)
Diabetes, *n* (%)	21 (7)
Family history, *n* (%)	96 (33)
Clinical history	
Chest pain, *n* (%)	95 (33)
Dyspnea, *n* (%)	20 (7)
Palpitation, *n* (%)	4 (1)
Positive stress test, *n* (%)	68 (24)
Follow-up of known CAD, *n* (%)	35 (12)
Valvular disease, *n* (%)	12 (4)
Arrhythmias, *n* (%)	43 (15)
Dilated cardiomyopathy, *n* (%)	11 (4)
Intravenous β-blocker	
Number of patients, *n* (%)	155 (54)
Dose (mg), mean ± SD	9.8 ± 4.7
Heart rate during the scan	
Minimum heart rate (bpm), mean ± SD	55.4 ± 9.6
Mean heart rate (bpm), mean ± SD	60.6 ± 10.5
Maximum heart rate (bpm), mean ± SD	74.4 ± 31.7
Radiation exposure	
Dose length product, mean ± SD	264.9 ± 125.5

CAD, coronary artery disease; SD, standard deviation.

Table 2
Comparison of Image Quality of all classes of patients by Readers 1 and 2.

	All classes		
	Reader 1	Reader 2	Cohen's Kappa
LM	3.2 ± 0.5	3.6 ± 0.5	0.93
Proximal_LAD	3.6 ± 0.5	3.6 ± 0.5	0.89
Mid_LAD	3.5 ± 0.6	3.5 ± 0.6	0.90
Distal_LAD	3.2 ± 0.8	3.1 ± 0.8	0.90
LAD	3.5 ± 0.6	3.5 ± 0.6	0.92
D1	2.9 ± 0.7	2.9 ± 0.7	0.89
Proximal_LCX	3.3 ± 0.6	3.3 ± 0.6	0.93
Mid_LCX	3.2 ± 0.7	3.2 ± 0.6	0.92
Distal_LCX	2.8 ± 0.8	2.8 ± 0.8	0.89
LCX	3.1 ± 0.6	3.1 ± 0.6	0.94
M1	2.8 ± 0.8	2.8 ± 0.8	0.93
Proximal_RCA	3.5 ± 0.6	3.5 ± 0.6	0.95
Mid_RCA	3.5 ± 0.6	3.5 ± 0.7	0.95
Distal_RCA	3.4 ± 0.7	3.4 ± 0.7	0.96
RCA	3.5 ± 0.6	3.5 ± 0.6	0.97
PLA	3.4 ± 0.6	3.3 ± 0.6	0.93
PDA	3.3 ± 0.7	3.3 ± 0.7	0.93
Patient	3.4 ± 0.6	3.4 ± 0.6	0.93

LM, left main coronary; LAD, anterior descending artery; D1, first diagonal artery; LCX, circumflex artery; M1, first obtuse marginal branch; RCA, right coronary artery, PLA, postero-lateral branch; PDA, posterior descending artery.

(53–79%), 91% (54–94%), 92% (89–96%), 63% (50–75%), 86% (82–90%), 89% (84–94%), respectively and 82% (76–88%), 58% (50–67%), 74% (66–82%), 69% (63–76%), 71% (66–76%), 78% (75–82%), respectively. The results concerning Model 1 and 2 are summarized in Table 4 and Fig. 4.

On multivariate analysis, the analysis tailored for plaque analysis showed that plaque characteristics, degree of stenosis as well as subjective image quality did not influence the predictive value of Model A (Table 5).

Considering that plaque imaging did not influence the diagnostic accuracy in Model A, we focused on plaque imaging in derived Model 1 and Model 2.

Table 3
Comparison of Image Quality of all classes of patients by the same Reader in two different lectures.

	All classes		
	First Lecture	Second Lecture	Cohen's Kappa
LM	3.2 ± 0.5	3.6 ± 0.5	0.90
Proximal_LAD	3.6 ± 0.5	3.6 ± 0.5	0.87
Mid_LAD	3.5 ± 0.6	3.5 ± 0.6	0.85
Distal_LAD	3.2 ± 0.8	3.1 ± 0.8	0.86
LAD	3.5 ± 0.6	3.5 ± 0.6	0.87
D1	2.9 ± 0.7	3.0 ± 0.7	0.86
Proximal_LCX	3.3 ± 0.6	3.3 ± 0.6	0.95
Mid_LCX	3.2 ± 0.7	3.1 ± 0.7	0.93
Distal_LCX	2.8 ± 0.8	2.7 ± 0.8	0.87
LCX	3.1 ± 0.6	3.1 ± 0.6	0.93
M1	2.8 ± 0.8	2.8 ± 0.8	0.91
Proximal_RCA	3.5 ± 0.6	3.5 ± 0.6	0.93
Mid_RCA	3.5 ± 0.6	3.5 ± 0.6	0.94
Distal_RCA	3.4 ± 0.7	3.4 ± 0.7	0.93
RCA	3.5 ± 0.6	3.5 ± 0.6	0.94
PLA	3.4 ± 0.6	3.3 ± 0.6	0.88
PDA	3.3 ± 0.7	3.2 ± 0.7	0.88
Patient	3.4 ± 0.6	3.4 ± 0.6	0.93

LM, left main coronary; LAD, anterior descending artery; D1, first diagonal artery; LCX, circumflex artery; M1, first obtuse marginal branch; RCA, right coronary artery, PLA, postero-lateral branch; PDA, posterior descending artery.

Regarding Models 1 and 2, multivariate analysis showed that the presence of plaque, regardless of the composition, was an independent predictor of success in Model 1; conversely, in Model 2, the presence of stenosis > 50% was a predictor of failure (Table 6).

After the evaluation of CCTA image quality and diagnostic accuracy of 2D CNN, we analyzed the impact of time consumed in terms of CAD-RADS classification and we observed that time of analysis was significantly higher ($p = 0.01$) for on-site physicians reading as compared to the CNN approach (530.5 ± 179.1 *vs.* 104.3 ± 1.4 sec, $p = 0.01$).

4. Discussion

Our study is the first to describe the application of AI for CAD-RADS classification. In clinical practice, it is important to correctly identify the CAD-RADS category. Patients in CAD-RADS 0 do not appear to derive benefit from medical therapy, while patients with CAD-RADS 1–2 may benefit from medical treatment and patients with CAD-RADS 3–5 may necessitate further testing of ischemia or invasive coronary angiography. The main results of our study are that Model A did not show a good diagnostic accuracy and area under the curve. A more simplified approach of CAD-RADS classification was shown in Model 1 and Model 2. Model 1 was composed of two subgroups of patients differing for clinical management based on CCTA results. As compared to Model A, Model 1 showed good diagnostic accuracy for detection of

Table 4
Diagnostic accuracy for Model 1 and Model 2.

	Model 1 (95%CI)	Model 2 (95%CI)
Sensitivity	66% (53–79%)	82% (76–88%)
Specificity	91% (87–95%)	58% (50–67%)
Positive predictive value	63% (50–75%)	69% (63–76%)
Negative predictive value	92% (89–96%)	74% (66–82%)
Accuracy	86% (82–90%)	71% (66–76%)
Area under curve	89% (84–94%)	78% (75–82%)
True positive	35	125
False positive	21	55
True negative	210	77
False negative	18	27

Model 1, CAD-RADS 0 *vs* CAD-RADS 1–5; Model 2, CAD-RADS 0–2 *vs* CAD-RADS 3-5.

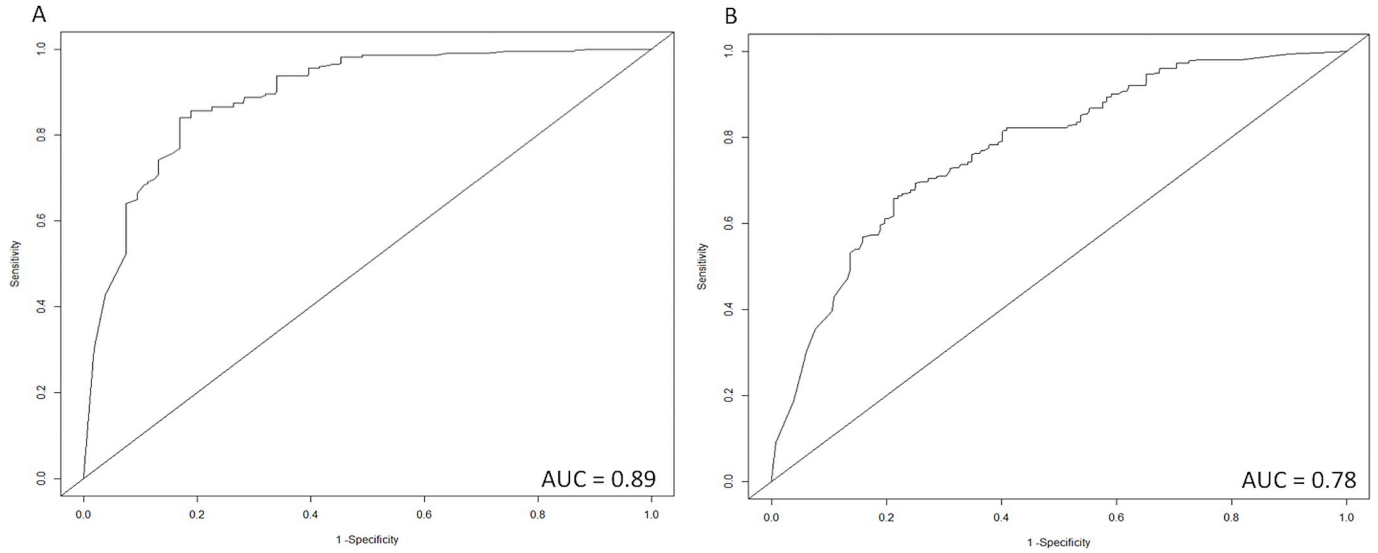

Fig. 4. Receiver operating characteristic curve (ROC) showing the predictive accuracy of Convolutional Neural Networks to distinguish between CAD-RADS 0 *vs.* CAD-RADS > 0 (Left Panel) and CAD-RADS 0–2 *vs*.CAD-RADS 3–5 (Model 2).

Table 5
Univariate analysis for model A.

CAD-RADS 0 *vs* CAD-RADS 1–2 *vs* CAD-RADS 3-5	Univariate	
	OR (95%CI)	*p* value
BMI	1.021(0.966–1.08)	0.455
Mean HR	0.992(0.969–1.017)	0.542
Plaques		
No plaques	–	–
Fibrotic	1.136(0.450–2.867)	0.787
Calcific	1.617(0.844–3.099)	0.147
Stenosis > 50%	1.269(0.743–2.057)	0.333
SNR	1.028(0.957–1.104)	0.447
CNR	1.020(0.95–1.094)	0.588

BMI, body mass index; HR, heart rate; SNR, signal to noise ratio; CNR, contrast to noise ratio.

patients positive and negative for the presence of CAD regardless of plaque composition and grade of stenosis. Finally, Model 2 was composed of two subgroups that mainly differ in the therapeutic approach after the results of CCTA. In the subgroup of CAD-RADS 0–2, patients may benefit from medical therapy while the subgroup of CAD-RADS 3–5 may benefit from further tests of ischemia or invasive coronary angiography [20]. Compared to Model 1, Model 2 showed a lower diagnostic accuracy and AUC with a high degree of stenosis as a major independent predictor of misclassification.

Nowadays, the non-invasive assessment of CAD is mainly focused on evaluation of calcium score (CS) and CCTA. Both CS and CCTA provide information useful for planning treatment strategy and prognostic stratification; therefore, considering the pivotal role of these CT acquisitions, an ML approach has been developed [7,21]. Artificial intelligence, similar to our manuscript, appears to be important for the diagnosis of CAD [22], furthermore, using some algorithms, it is possible also to provide information concerning CAD in non-gated CT images [23].

Takx et al. described the possibility to evaluate CS using non-contrast, non-gated CT using a low dose protocol [23]. In particular, Takx and colleagues, using a supervised pattern recognition system k-nearest neighbor with support vector machine classifiers for identification of CS, demonstrated a good reliability when compared with CS calculated by manual delineation [23].

One of the applications of AI in CCTA was shown by Kang and colleagues [22]. The authors, using a two-step ML approach which incorporated a support vector machine, demonstrated a sensitivity, specificity, accuracy and AUC of 93%; 95%, 94% and 94%, in diagnosing CAD. This promising technique did not differentiate the entity of CAD further and the authors did not specify the time spent for each analysis [22]. Another interesting technique for the evaluation of CAD in CCTA using an automated algorithm was described by Dey et al. [24]. The authors quantified the non-calcified and calcified plaque using an automated algorithm and discovered a good agreement when compared with human evaluation [24].

The aforementioned manuscripts regarding the application of AI in diagnostic pathway of CAD differ by the algorithm of AI used. Despite we used the 2D CNN approach, unlike the others articles that used different algorithms of AI, we have in common the main purpose represented by the simplification of diagnostic pathway.

Despite the aforementioned studies analyzing the impact of AI in cardiac imaging, none of them evaluate its role in CAD-RADS classification.

In this article, the main finding is represented by the ability of CNN to differentiate with high diagnostic accuracy patients with CAD-RADS 0 *versus* CAD-RADS > 0.

Based on the results of our manuscript, it may be possible to use a CNN algorithm in clinical practice and rule out the presence of CAD in a relatively short time. Considering that the prevalence of normal coronaries is high in patients even with an increased pretest probability [25,26], it is plausible that CCTA interpretation may be accelerated by the application of CNN algorithms as shown in Fig. 5.

Another important finding is the possibility to correctly predict with high diagnostic accuracy Models 1 and 2, independently of the image quality of CCTA acquisition. Indeed, both SNR and CNR do not appear to influence CAD-RADS classification using CNN. The latter finding is important, especially when employing low dose CCTA protocols.

Some limitations should be mentioned in this manuscript.

First, a small sample size was used for the study. A larger, multicenter study, involving a larger sample size may increase the diagnostic accuracy in all three models used in the manuscript.

Second, we speculate that for Model 1, the CNN approach was able to better identify patients with plaque because an increase in CAD-RADS score is correlated with more calcified and soft plaque and subsequently a larger amount of data for the training set.

Third, most of the CCTA were acquired using the latest generation CT, therefore it is important to consider that the application of CNN algorithms may provide different results with poor image quality.

In conclusion, this new CNN approach can be helpful for the identification of patients with CAD-RADS 0 in a short time of analysis using

Table 6
Univariate and multivariate analysis for Model 1 and 2.

Model 1 (CAD-RADS 0 *vs* CAD-RADS 1–5)				
	Univariate		**Multivariate**	
	OR (95%CI)	***p* value**	**OR (95%CI)**	***p* value**
BMI	0.987 (0.909–1.073)	0.762		
Mean HR	0.995 (0.962–1.03)	0.775		
Plaques				
No plaque	–	–	–	–
Fibrotic	**0.125(0.027–0.581)**	**0.008**	0.142(0.030–0.671)	0.014
Calcific	**0.216(0.103–0.451)**	**< 0.001**	0.291(0.121–0.701)	0.002
Stenosis > 50%	**0.351(0.164–0.751)**	**0.007**	0.592(0.236–1.481)	0.262
SNR	1.066 (0.968–1.175)	0.196		
CNR	1.064 (0.967–1.171)	0.202		
Model 2 (CAD-RADS 0–2 *vs* CAD-RADS 3–5)				
	Univariate		**Multivariate**	
	OR (95%CI)	***p* value**	**OR (95%CI)**	***p* value**
BMI	1.038 (0.979–1.100)	0.217		
Mean HR	0.998 (0.973–1.024)	0.893		
Plaque				
No plaque	–	–	–	–
Fibrotic	2.074 (0.632–6.804)	0.229	1.511(0.445–5.132)	0.508
Calcific	**4.381(1.785–10.754)**	**0.001**	2.420(0.896–6.534)	0.081
Stenosis > 50%	**3.350(1.949–5.759)**	**< 0.001**	2.476(1.349–4.543)	0.003
SNR	0.984 (0.911–1.063)	0.684		
CNR	0.980 (0.909–1.058)	0.606		

BMI, body mass index; HR, heart rate; SNR, signal to noise ratio; CNR, contrast to noise ratio.

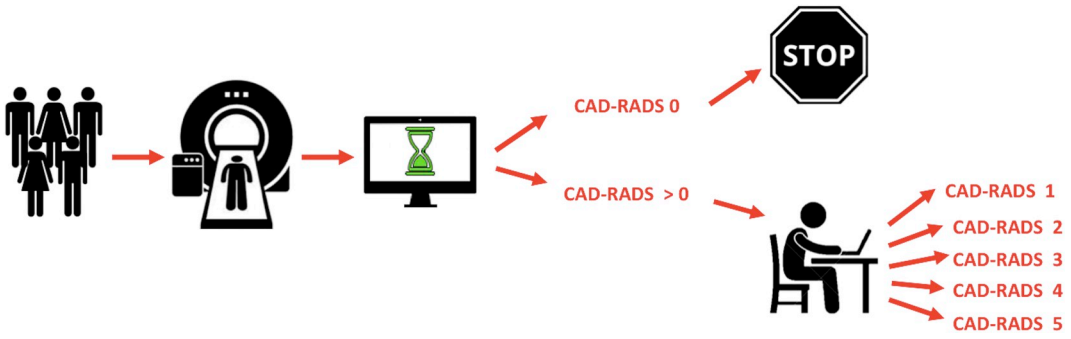

Fig. 5. Simulation of the diagnostic algorithm in a clinical setting using CNN for CAD-RADS classification.

a good image quality dataset. Further studies with a larger population need to be performed to improve the diagnostic accuracy of CNN.

Authors contribution

Giuseppe Muscogiuri, Mattia Chiesa, Gianluca Pontone: Conceptualization, Methodology and Writing Original Data, Supervision. Michela Trotta: Software, Marco Gatti, Vitanio Palmisano, Serena Dell'Aversana, Francesca Baessato, Annachiara Cavaliere, Gloria Cicala, Antonella Loffreno, Giulia Rizzon: Data Curation, Data collecting and Data analysis Marco, Guglielmo, Andrea Baggiano, Laura Fusini, Luca Saba, Daniele Andreini, Mauro Pepi, Andrea Guaricci and Carlo De Cecco: Methodology, Mark G. Rabbat: Writing, Gualtiero Colombo: Supervision.

Declaration of competing interest

The authors declared they do not have anything to disclose regarding conflict of interest with respect to this manuscript.

Acknowledgements

Study Fundings. Italian Ministry of Health, Rome, Italy (RC 2017 R1061/19-CCM1125).

Appendix A. Supplementary data

Supplementary data to this article can be found online at https://doi.org/10.1016/j.atherosclerosis.2019.12.001.

.

References

[1] G. Pontone, D. Andreini, A.L. Bartorelli, S. Cortinovis, S. Mushtaq, E. Bertella, A. Annoni, A. Formenti, E. Nobili, D. Trabattoni, P. Montorsi, G. Ballerini, P. Agostoni, M. Pepi, Diagnostic accuracy of coronary computed tomography angiography: a comparison between prospective and retrospective electrocardiogram triggering, J. Am. Coll. Cardiol. 54 (2009) 346–355.

[2] G. Pontone, D. Andreini, A.L. Bartorelli, E. Bertella, S. Cortinovis, S. Mushtaq, C. Foti, A. Annoni, A. Formenti, A. Baggiano, E. Conte, F. Bovis, F. Veglia, G. Ballerini, C. Fiorentini, P. Agostoni, M. Pepi, A long-term prognostic value of CT angiography and exercise ECG in patients with suspected CAD, JACC Cardiovasc Imaging 6 (2013) 641–650.

[3] G. Pontone, A. Baggiano, D. Andreini, A.I. Guaricci, M. Guglielmo, G. Muscogiuri, L. Fusini, F. Fazzari, S. Mushtaq, E. Conte, G. Calligaris, S. De Martini, C. Ferrari, S. Galli, L. Grancini, P. Ravagnani, G. Teruzzi, D. Trabattoni, F. Fabbiocchi, A. Lualdi, P. Montorsi, M.G. Rabbat, A.L. Bartorelli, M. Pepi, Stress computed tomography perfusion versus fractional flow reserve CT derived in suspected coronary artery disease: the PERFECTION study, JACC Cardiovasc Imaging 12 (2019) 1487–1497.

[4] R.C. Cury, S. Abbara, S. Achenbach, A. Agatston, D.S. Berman, M.J. Budoff, K.E. Dill, J.E. Jacobs, C.D. Maroules, G.D. Rubin, F.J. Rybicki, U.J. Schoepf, L.J. Shaw, A.E. Stillman, C.S. White, P.K. Woodard, J.A. Leipsic, CAD-RADS(TM)

coronary artery disease - reporting and data system. An expert consensus document of the society of cardiovascular computed tomography (SCCT), the American college of radiology (ACR) and the north American society for cardiovascular imaging (NASCI). Endorsed by the American college of cardiology, J Cardiovasc Comput Tomogr 10 (2016) 269–281.

[5] J.X. Xie, R.C. Cury, J. Leipsic, M.T. Crim, D.S. Berman, H. Gransar, M.J. Budoff, S. Achenbach, O.H. B, T.Q. Callister, H. Marques, R. Rubinshtein, M.H. Al-Mallah, D. Andreini, G. Pontone, F. Cademartiri, E. Maffei, K. Chinnaiyan, G. Raff, M. Hadamitzky, J. Hausleiter, G. Feuchtner, A. Dunning, A. DeLago, Y.J. Kim, P.A. Kaufmann, T.C. Villines, B.J.W. Chow, N. Hindoyan, M. Gomez, F.Y. Lin, E. Jones, J.K. Min, L.J. Shaw, The coronary artery disease-reporting and data system (CAD-RADS): prognostic and clinical implications associated with standardized coronary computed tomography angiography reporting, JACC Cardiovasc Imaging 11 (2018) 78–89.

[6] G. Chartrand, P.M. Cheng, E. Vorontsov, M. Drozdzal, S. Turcotte, C.J. Pal, S. Kadoury, A. Tang, Deep learning: a primer for radiologists, RadioGraphics 37 (2017) 2113–2131.

[7] S.J. Al'Aref, K. Anchouche, G. Singh, P.J. Slomka, K.K. Kolli, A. Kumar, M. Pandey, G. Maliakal, A.R. van Rosendael, A.N. Beecy, D.S. Berman, J. Leipsic, K. Nieman, D. Andreini, G. Pontone, U.J. Schoepf, L.J. Shaw, H.J. Chang, J. Narula, J.J. Bax, Y. Guan, J.K. Min, Clinical applications of machine learning in cardiovascular disease and its relevance to cardiac imaging, Eur. Heart J. (2018).

[8] G. Litjens, T. Kooi, B.E. Bejnordi, A.A.A. Setio, F. Ciompi, M. Ghafoorian, J. van der Laak, B. van Ginneken, C.I. Sanchez, A survey on deep learning in medical image analysis, Med. Image Anal. 42 (2017) 60–88.

[9] G. Pontone, G. Muscogiuri, D. Andreini, A.I. Guaricci, M. Guglielmo, A. Baggiano, F. Fazzari, S. Mushtaq, E. Conte, A. Annoni, A. Formenti, E. Mancini, M. Verdecchia, A. Campari, C. Martini, M. Gatti, L. Fusini, L. Bonfanti, E. Consiglio, M.G. Rabbat, A.L. Bartorelli, M. Pepi, Impact of a new adaptive statistical iterative reconstruction (ASIR)-V algorithm on image quality in coronary computed tomography angiography, Acad. Radiol. 25 (2018) 1305–1313.

[10] R.A. Takx, D. Sucha, J. Park, T. Leiner, U. Hoffmann, Sublingual nitroglycerin administration in coronary computed tomography angiography: a systematic review, Eur. Radiol. 25 (2015) 3536–3542.

[11] G. Pontone, D. Andreini, A.L. Bartorelli, E. Bertella, S. Mushtaq, C. Foti, A. Formenti, L. Chiappa, A. Annoni, S. Cortinovis, A. Baggiano, E. Conte, F. Bovis, F. Veglia, G. Ballerini, P. Agostoni, C. Fiorentini, M. Pepi, Feasibility and diagnostic accuracy of a low radiation exposure protocol for prospective ECG-triggering coronary MDCT angiography, Clin. Radiol. 67 (2012) 207–215.

[12] G. Pontone, G. Muscogiuri, A. Baggiano, D. Andreini, A.I. Guaricci, M. Guglielmo, F. Fazzari, S. Mushtaq, E. Conte, A. Annoni, A. Formenti, E. Mancini, M. Verdecchia, L. Fusini, L. Bonfanti, E. Consiglio, M.G. Rabbat, A.L. Bartorelli, M. Pepi, Image quality, overall evaluability, and effective radiation dose of coronary computed tomography angiography with prospective electrocardiographic triggering plus intracycle motion correction algorithm in patients with a heart rate over 65 beats per minute, J. Thorac. Imaging 33 (2018) 225–231.

[13] G. Pontone, D. Andreini, E. Bertella, A. Baggiano, S. Mushtaq, M. Loguercio, C. Segurini, E. Conte, V. Beltrama, A. Annoni, A. Formenti, M. Petulla, A.I. Guaricci, P. Montorsi, D. Trabattoni, A.L. Bartorelli, M. Pepi, Impact of an intra-cycle motion correction algorithm on overall evaluability and diagnostic accuracy of computed tomography coronary angiography, Eur. Radiol. 26 (2016) 147–156.

[14] T. Pflederer, L. Rudofsky, D. Ropers, S. Bachmann, M. Marwan, W.G. Daniel, S. Achenbach, Image quality in a low radiation exposure protocol for retrospectively ECG-gated coronary CT angiography, AJR Am. J. Roentgenol. 192 (2009) 1045–1050.

[15] W.G. Austen, J.E. Edwards, R.L. Frye, G.G. Gensini, V.L. Gott, L.S. Griffith, D.C. McGoon, M.L. Murphy, B.B. Roe, A reporting system on patients evaluated for coronary artery disease. Report of the Ad Hoc committee for grading of coronary artery disease, council on cardiovascular surgery, American heart association, Circulation 51 (1975) 5–40.

[16] F. Cademartiri, M. Romano, S. Seitun, E. Maffei, A. Palumbo, M. Fusaro, A. Aldrovandi, G. Messalli, S. Tresoldi, R. Malago, L. La Grutta, G. Runza, V. Brambilla, C. Tedeschi, G. Casolo, M. Midiri, N.R. Mollet, Prevalence and characteristics of coronary artery disease in a population with suspected ischemic heart disease using CT coronary angiography: correlations with cardiovascular risk factors and clinical presentation, Radiol. Med. 113 (2008) 363–372.

[17] J. Leipsic, S. Abbara, S. Achenbach, R. Cury, J.P. Earls, G.J. Mancini, K. Nieman, G. Pontone, G.L. Raff, SCCT guidelines for the interpretation and reporting of coronary CT angiography: a report of the Society of Cardiovascular Computed Tomography Guidelines Committee, J Cardiovasc Comput Tomogr 8 (2014) 342–358.

[18] S. Pereira, A. Pinto, V. Alves, C.A. Silva, Brain tumor segmentation using convolutional neural networks in MRI images, IEEE Trans. Med. Imaging 35 (2016) 1240–1251.

[19] J.J. Nirschl, A. Janowczyk, E.G. Peyster, R. Frank, K.B. Margulies, M.D. Feldman, A. Madabhushi, A deep-learning classifier identifies patients with clinical heart failure using whole-slide images of H&E tissue, PLoS One 13 (2018) e0192726.

[20] G. Pontone, D. Andreini, A.I. Guaricci, A. Baggiano, F. Fazzari, M. Guglielmo, G. Muscogiuri, C.M. Berzovini, A. Pasquini, S. Mushtaq, E. Conte, G. Calligaris, S. De Martini, C. Ferrari, S. Galli, L. Grancini, P. Ravagnani, G. Teruzzi, D. Trabattoni, F. Fabbiocchi, A. Lualdi, P. Montorsi, M.G. Rabbat, A.L. Bartorelli, M. Pepi, Incremental diagnostic value of stress computed tomography myocardial perfusion with whole-heart coverage CT scanner in intermediate- to high-risk symptomatic patients suspected of coronary artery disease, JACC Cardiovasc Imaging 12 (2019) 338–349.

[21] G. Singh, S.J. Al'Aref, M. Van Assen, T.S. Kim, A. van Rosendael, K.K. Kolli, A. Dwivedi, G. Maliakal, M. Pandey, J. Wang, V. Do, M. Gummalla, C.N. De Cecco, J.K. Min, Machine learning in cardiac CT: basic concepts and contemporary data, J Cardiovasc Comput Tomogr 12 (2018) 192–201.

[22] D. Kang, D. Dey, P.J. Slomka, R. Arsanjani, R. Nakazato, H. Ko, D.S. Berman, D. Li, C.C. Kuo, Structured learning algorithm for detection of nonobstructive and obstructive coronary plaque lesions from computed tomography angiography, J. Med. Imaging 2 (2015) 014003.

[23] R.A. Takx, P.A. de Jong, T. Leiner, M. Oudkerk, H.J. de Koning, C.P. Mol, M.A. Viergever, I. Isgum, Automated coronary artery calcification scoring in non-gated chest CT: agreement and reliability, PLoS One 9 (2014) e91239.

[24] D. Dey, V.Y. Cheng, P.J. Slomka, R. Nakazato, A. Ramesh, S. Gurudevan, G. Germano, D.S. Berman, Automated 3-dimensional quantification of noncalcified and calcified coronary plaque from coronary CT angiography, J Cardiovasc Comput Tomogr 3 (2009) 372–382.

[25] B.J. Chow, G. Small, Y. Yam, L. Chen, S. Achenbach, M. Al-Mallah, D.S. Berman, M.J. Budoff, F. Cademartiri, T.Q. Callister, H.J. Chang, V. Cheng, K.M. Chinnaiyan, A. Delago, A. Dunning, M. Hadamitzky, J. Hausleiter, P. Kaufmann, F. Lin, E. Maffei, G.L. Raff, L.J. Shaw, T.C. Villines, J.K. Min, C. Investigators, Incremental prognostic value of cardiac computed tomography in coronary artery disease using CONFIRM: COroNary computed tomography angiography evaluation for clinical outcomes: an InteRnational Multicenter registry, Circ Cardiovasc Imaging 4 (2011) 463–472.

[26] B. Foldyna, J.E. Udelson, J. Karady, D. Banerji, M.T. Lu, T. Mayrhofer, D.O. Bittner, N.M. Meyersohn, H. Emami, T.S.S. Genders, C.B. Fordyce, M. Ferencik, P.S. Douglas, U. Hoffmann, Pretest probability for patients with suspected obstructive coronary artery disease: re-evaluating Diamond-Forrester for the contemporary era and clinical implications: insights from the PROMISE trial, Eur Heart J Cardiovasc Imaging (2018).